Terahertz Sensor for Non-Contact Thickness and Quality Measurement of Automobile Paints of Varying Complexity

Ke Su, Yao-Chun Shen, and J. Axel Zeitler

***Abstract*—In this paper, we propose to use terahertz pulsed imaging (TPI) as a novel tool to measure the thickness and quality of up to four layers of car paint on both metallic and non-metallic substrates. Using a rigorous one-dimensional electromagnetic model for terahertz propagation in a multi-layered medium combined with a numerical fitting method, the refractive index, extinction coefficient, and thickness of individual paint layers were determined. This proposed method was shown to be able to resolve coating layers down to a thickness of 18 μm and was validated for both single- and multi-layer automobile paint samples. Results of the terahertz measurements were benchmarked against other techniques that are currently used for non-destructive testing during car manufacture: ultrasound and eddy current measurements, as well as two reference techniques, X-ray microcomputed tomography and surface profilometry. Good consistency was found between the techniques. Compared to conventional techniques, TPI has the advantage that it is a non-contact method and that it is able to spatially resolve the thickness uniformity distribution information by two-dimensional mapping.**

***Index Terms*—Optical properties, optical time domain reflectometry, terahertz imaging, thin films.**

I. Introduction

RECENT developments in terahertz time-domain spectroscopy have opened up a number of opportunities for non-destructive testing applications across a large range of fields [1], including nondestructive evaluation of aircraft materials [2], pharmaceutical tablet properties testing [3]–[5], and explosives detection [6], [7]. A further, yet largely unexplored, application of terahertz sensing is in non-destructive testing of paint layers in the automotive industry. Painting is a very important processing step during automotive manufacturing. Paint coats perform a number of important functions, not only by giving distinct colors to a vehicle, but also by providing crucial protection from UV radiation, corrosion, scratches, and harmful chemicals.

Conventional methods to measure the thickness of car paint layers that are commercially available, such as magnetic gauges,[1] eddy current measurements,[2] and ultrasound testing[3] all require direct contact between the measurement sensor and the painted car surface. These measurement techniques can only cover a limited number of sampling points on selected cars and hence lack the capability to identify paint defects, monitor drying processes and map the thickness distribution of the paint layers over a larger surface of the vehicle. Both magnetic gauges and eddy current measurements can only be used when measuring the thickness of paint layers on metal substrates. In addition, only the ultrasound technique is capable of resolving individual layers whereas the other techniques merely measure total thickness of the film build.

Terahertz-based measurement systems have recently been introduced as a technology for measuring car paint thickness and quality. Yasui *et al.* [8] demonstrated a terahertz "paintmeter" for non-contact mapping of the thickness of both single layer and two-layer paints with relatively thick film builds (above 100 μm). Yasuda *et al.* [9] proposed a numerical parameter fitting method which increases the sensitivity of the minimum thickness measurement. For simplicity of parameter fitting, the physics model neglected the effects of dispersion in refractive index, absorption of the paint, and multiple reflections in the terahertz pulse. However, thin film paint layers will result in multiple reflections of the signal inside the sample and consequently the time-domain trace of the sample signal will contain a sequence of signal echoes following the main reflected pulse, which is particularly noticeable in the case of multiple paint layers on a metallic substrate.

In this paper, a rigorous one-dimensional (1-D) electromagnetic model for terahertz propagation in a multilayered medium is used to simulate reflected terahertz pulses. Given the complex dielectric function of individual layers in a multi-layer structure, the reflection coefficients are calculated at each frequency using this electromagnetic model. After applying an appropriate filter function, the calculated reflection coefficients are inverse Fourier transformed back to the time-domain to obtain the simulated reflected terahertz waveform. Refractive indices, extinction coefficients and thickness of each individual layer of the

Manuscript received March 19, 2014; revised May 13, 2014; accepted May 14, 2014. Date of publication June 06, 2014; date of current version June 26, 2014. This work was supported in part by the Technology Strategy Boardunder Award 101262, and by the U.K. Engineering and Physical Sciences Research Council under EP/K503721/1.

K. Su and J. A. Zeitler are with the Department of Chemical Engineering and Biotechnology, University of Cambridge, Cambridge CB2 3RA, U.K. (e-mail: ks665@cam.ac.uk; jaz22@cam.ac.uk).

Y.-C. Shen is with the Department of Electrical Engineering and Electronics, University of Liverpool, Liverpool L69 3GJ, U.K. (e-mail: y.c.shen@liverpool.ac.uk).

Color versions of one or more of the figures in this paper are available online at http://ieeexplore.ieee.org.

Digital Object Identifier 10.1109/TTHZ.2014.2325393

[1]http://www.defelsko.com

[2]http://www.elcometer.com

[3]http://www.jsrultrasonics.com/coatthicksystems.html

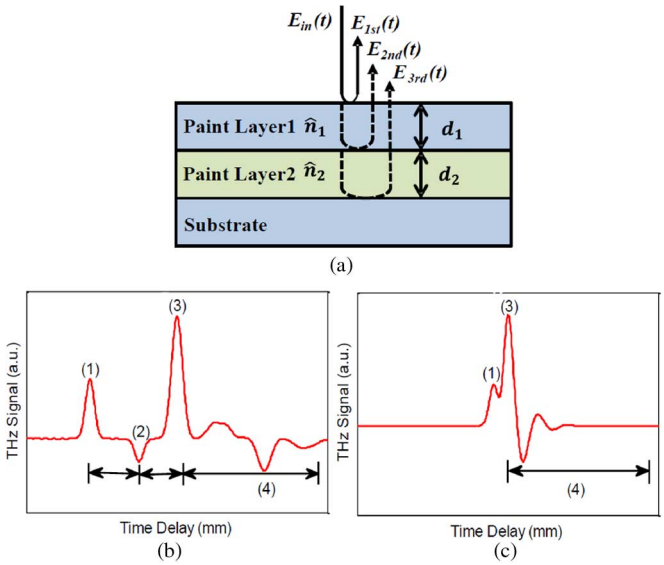

Fig. 1. (a) Principle of the multiple paint layer thickness measurement by terahertz pulsed reflection. (b) Schematic diagram of a reflected terahertz waveform from an optically thick sample where all reflected pulses are well separated in time. (c) Schematic diagram of a reflected terahertz waveform from an optically thin sample. Multiple reflection peaks are observed: (1) reflection from air to paint layer 1 interface;, (2) reflection from paint layer 1 to paint layer 2 interface; (3) reflection from paint layer 2 to substrate; (4) multiple etalon reflections.

sample can be determined by a numerical parameter fitting algorithm. In order to validate the ability of this method to evaluate the thickness and uniformity of car paint films, the thickness of single- and multi-layer paint samples, consisting of up to four different layers covering a range of typical coating patterns used in the automotive industry, were measured by terahertz pulsed imaging (TPI) using a TPS Spectra 3000 with reflection imaging module (TeraView Ltd., Cambridge, U.K.) and compared with the currently used reference techniques such as: profilometer (Talysurf i120, Leicester, U.K.), ultrasound (μP501A PELT, Imaginant Inc, NY, USA), eddy current measurement (Elcometer 456, Elcometer Limited, Edge Lane, U.K.), as well as X-ray microcomputed tomography (XμCT, Skyscan 1172, Kontich, Belgium). The TPI results show good agreement with the other methods.

II. Principle

For clarity the following discussion of the coating thickness extraction technique considers only two paint layers on a substrate. However, the same principle is employed to describe additional layers in the remainder of the paper. The substrate upon which the paint layers are deposited can either be metallic (e.g., aluminum or steel) or non-metallic (e.g. carbon fiber, plastic, etc.). For each paint layer the refractive index, extinction coefficient and thickness are described by $\hat{n}_1 = n_1 + i\kappa_1$, $\hat{n}_2 = n_2 + i\kappa_2$ and d_1, d_2 respectively.

When a terahertz pulse is incident on an automotive panel, reflections arise in the terahertz waveform whenever there is a change of the sample microstructure, which causes a change in the refractive index and/or extinction coefficient of the material (Fig. 1).

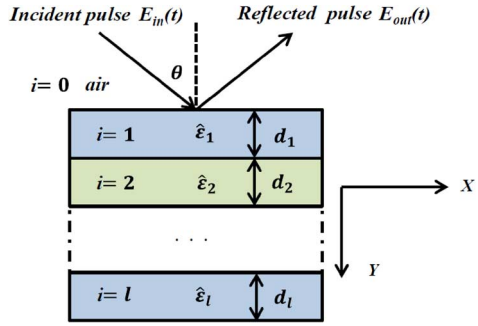

Fig. 2. 1-D electromagnetic model for terahertz propagation into and reflection from a multi-layer medium.

A. Optically Thick Samples

In the case of optically thick samples all peaks due to reflection from an interface between adjacent layers are well separated [Fig. 1(b)]. For pulses propagating at normal incidence, the layer thickness can be calculated directly from the time delay between neighboring reflections as follows:

$$d_1 = \frac{\Delta t_{12}}{2n_1} \tag{1}$$

$$d_2 = \frac{\Delta t_{23}}{2n_2} \tag{2}$$

where Δt_{12} and Δt_{23} are the time separations expressed as optical delay in mm between the reflection pulses [10], [11].

As shown in Fig. 1(b), the first reflection is due to the interface between free space (air, $n_0 = 1$) and the first paint layer. The refractive index of the first layer, n_1 is greater than the refractive index of the preceding medium and hence a positive peak is observed. In this example $n_2 < n_1$ and hence a negative peak corresponds to the reflection from the boundary between layers 1 and 2. The third reflection peak originates from the interface between layer 2 and the substrate and is positive since $n_{\text{substrate}} > n_2$. Region 4 contains the multiple etalon reflections originating from the paints layers.

B. Optically Thin Samples

For optically thin paint layers reflection peaks from layer interfaces are not well separated in the time-domain which means that the layer thickness cannot be extracted using the above peak separation method [Fig. 1(c)]. In order to be able to quantify thin coating layers we have developed a signal processing algorithm based on the 1-D propagation of the electromagnetic field to resolve and extract the individual layer thickness of multiple paint layers (Fig. 2).

1) 1-D Propagation Model: A detailed derivation of the underlying model was presented earlier [11], but given the importance of the model to the following implementation in the thickness extraction algorithm we briefly introduce the key concept of the method. Given that we know the number of layers present in the sample, l, we specify their number in this implementation of the model and we also limit the model to p polarization of the incident light as is the case for our experimental setup. We furthermore make the assumption that the optical properties of each layer are uniform in the transverse direction.

In the 1-D propagation model each layer i is characterized by a dielectric function $\hat{\epsilon}_i(v)$ and thickness d_i. The z-component of the magnetic field can be expressed as

$$H_z^{(i)}(x,y) = A_i \exp\left(j(ax - b_i y)\right) + B_i \exp\left(j(ax + b_i y)\right), \quad i = 0, 1, 2 \ldots, l \quad (3)$$

where A_i is the transmitted amplitude and B_i is the reflected amplitude of layer i, and

$$a = \sqrt{\hat{\epsilon}_1(v)} k_0 \sin(\theta) \quad (4)$$

$$b_i = \sqrt{\hat{\epsilon}_i(v) k_0^2 - a^2}. \quad (5)$$

Here k_0 is the wavenumber of light in vacuum and θ is the angle of incidence of the terahertz pulse. Using Maxwell's equation the x-component of the electric field can be obtained:

$$E_x^{(i)}(x,y) = \frac{1}{j\omega\hat{\epsilon}_i(v)} \frac{\partial \left[H_z^{(i)}(x,y)\right]}{\partial y}. \quad (6)$$

At the boundary of $y = d_i$, continuity is observed in $H_z^{(i)}(x,y)$ and $E_x^{(i)}(x,y)$:

$$H_z^{(i)}(x,d_i) = H_z^{(i+1)}(x,d_i) \quad (7)$$

$$E_x^{(i)}(x,d_i) = E_x^{(i+1)}(x,d_i), \qquad i = 0, 1, 2, \ldots, l-1 \quad (8)$$

This allows us to develop the following expression for A_i and B_i:

$$A_i = \frac{\exp(j\beta_i d_i)}{2} \left[A_{i+1} \exp(-j\beta_{i+1} d_i)(1 + \tau_i) + B_{i+1} \exp(j\beta_{i+1} d_i)(1 - \tau_i)\right] \quad (9)$$

$$B_i = \frac{\exp(j\beta_i d_i)}{2} \left[A_{i+1} \exp(-j\beta_{i+1} d_i)(1 - \tau_i) + B_{i+1} \exp(j\beta_{i+1} d_i)(1 + \tau_i)\right] \quad (10)$$

where $\tau_i = \hat{\epsilon}_i(v)\beta_{i+1}/\hat{\epsilon}_{i+1}(v)\beta_i$.

We explicitly take into account the frequency dependence of $\hat{\epsilon}_i(v)$ for each layer, by implementing this in terms of the complex index of refraction $\hat{n}_i(v) = \sqrt{\hat{\epsilon}_i(v)}$. The complex refractive index is defined as

$$\hat{n}(v) = n_{\text{eff}}(v) + i\kappa(v) \quad (11)$$

where $n_{\text{eff}}(v)$ is the effective refractive index and $\kappa(v)$ is the extinction coefficient. In our model for typical automotive paints we approximate the real part of the refractive index n_{eff} to be constant at terahertz frequencies, while we assume that $\kappa(v)$ increases linearly with frequency as

$$\kappa(v) = \kappa_{\text{eff}} v. \quad (12)$$

For polymer based car paints that do not contain particles that lead to appreciable scattering effects we found these two assumptions suitable to approximate the optical properties of the paint layers [12]. In order to account for scattering effects (12) can be modified to the power of two [13]. Other models for $\hat{n}(v)$ can be easily used instead to account for the dielectric properties of different materials.

Using the optical properties defined by (11) and (12) and initial guessed values of thickness for each layer, A_0 and B_0 can be obtained by iteration. The reflection coefficient $R(v)$ can be calculated as the ratio of the reflected amplitude B_0 to the incident amplitude A_0:

$$R(v) = \left|\frac{B_0}{A_0}\right|. \quad (13)$$

2) Simulation of Reflected Waveform: The incident time-domain terahertz pulse is Fourier transformed into the frequency-domain, $E_{\text{ref}}(v)$. Then the reflected complex amplitude spectrum $E_{\text{out}}(v)$ is obtained using the Fourier transformed time-domain waveform of a reference waveform acquired from a mirror $E_{\text{ref}}(v)$ and the reflectance coefficient $R(v)$ calculated in (13) by

$$E_{\text{out}}(v) = E_{\text{ref}}(v) \times R(v). \quad (14)$$

Finally, the calculated reflected complex amplitude spectra $E_{\text{out}}(v)$ were Fourier transformed back to the time domain to obtain the simulated reflected terahertz waveform.

3) Layer Thickness Extraction From Experimental Waveform: The thickness of each coating layer was then extracted by fitting the measured reflected waveform with the simulated waveform by iterating d_i and minimizing the residual sum of squares between the measured and simulated waveforms using the least square method.

III. Samples Measurements

A. Paint Samples

For this study, three sets of automobile paint samples with different layer configurations were prepared, as depicted in Fig. 3. The first set of paint samples are single layer paints coated over one half of a flat mirror of dimensions 25×25 mm. The thickness of the single-layer paint film was measured independently using a mechanical stylus profilometer, from which the optical properties (refractive index and extinction coefficient) of different paints were determined using the numerical optimization routine outlined above. Based on these single layer calibration samples, a library of terahertz properties was built for the different paint samples, which was used for the subsequent analysis of multi-layer paint samples of unknown thickness.

The second set of paint samples are designed to be representative of typical automotive paint layer structures used for painting metal body panels. These samples contain four layers of automotive paints applied onto a flat metallic substrate as shown in Fig. 3(b). The four layers are: electrocoat, primer, a pigmented basecoat and finally a pigment free clear polymer layer (clearcoat) in the order applied to the metal substrate. The thickness of each of these layers typically ranges from 10 to 100 μm, depending on the coating function, with a typical total film build of 170–240 μm. Each layer performs a different function: The first layer applied to a metal substrate is the electrocoat, which is applied using an electrochemical reaction and provides corrosion protection of the metal substrate. The primer is designed to promote adhesion between the electrocoat and the

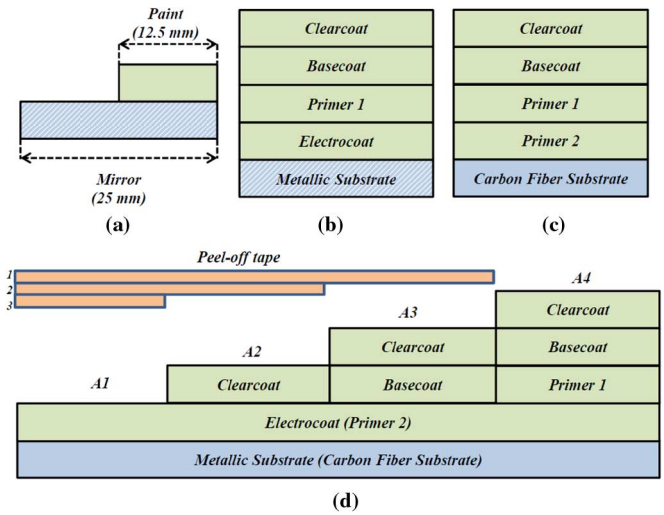

Fig. 3. Cross-sectional schematic of the automobile paint samples used in this study. (a) Single-layer paint film on an optically flat mirror substrate. (b) Four-layer automobile paint on metallic substrate. (c) Four-layer automobile paint on carbon fiber substrate. (d) Four step paint sample on both metallic and carbon fiber substrate (A1: one-layer paint, A2: two-layer paint, A3: three-layer paint and A4: four-layer paint).

layers above and also serves to smooth out surface roughness originating from the electrocoat. The final two layers of the paint system, the basecoat and clearcoat, comprise what is often referred to as the top-coat. The basecoat is the layer that provides color to the paint system, which contains organic, inorganic, and special effect pigments (such as aluminum flakes, micas) that give a vehicle its particular color. To protect these pigments from the environment, a glossy and transparent clearcoat is applied over the color basecoat. The clearcoat offers protection from UV radiation, mechanical scratches and resistance against chemical corrosion and is typically the thickest layer.

In addition to metal substrates, carbon fiber composite materials are increasingly being used in the automotive industry due to their high stiffness, ultra-lightweight and corrosion resistance properties compared to metals such as steel and aluminum. The final set of paint samples comprises a full stack of four layers of automotive paint on a carbon fiber substrate. For this type of substrate a layer of conductive primer paint is applied (primer 2), instead of electrocoat, to ensure electrical conductivity of the substrate, which is essential to allow electrostatic spray paint operation on carbon fiber substrates.

Both sets of paint samples, stack 2 [Fig. 3(b)\ and stack 3 [Fig. 3(c)] were prepared by applying a stepped paint layer structure [as shown schematically in Fig. 3(d)] onto a 8 × 12 cm rectangular substrate. Three layers of peel-off tapes (1, 2 and 3) were first applied to cover the base paint layer applied on the substrate. (electrocoat for metallic substrate and primer 2 for carbon fiber substrate). The step structures (A1, A2, A3, and A4) were achieved by peeling off the respective tapes in order during the painting process. Using this strategy, the thickness for each kind of paint layer remains the same for each step and the individual thickness of each layer of the full stack sample can be determined even for the eddy current meter measurement by simple subtraction, i.e. the thickness of the clearcoat layer $d_{\mathrm{clear}} = d_{A2} - d_{A1}$.

B. Terahertz Pulsed Imaging (TPI)

TPI measurements of paint samples were acquired in reflection mode with an angle of incidence of 30 degrees to the normal using a commercial TPI system (TPS Spectra 3000 system with reflection imaging module, TeraView Ltd., Cambridge, U.K.). The system has a useful spectral range of 60 GHz–3.6 THz, corresponding to a wavelength range of 0.08–5 mm. The detailed description of the TPI system was presented earlier [14]. In brief, a beam splitter separates a femtosecond pulse of near-infrared (NIR) laser light into an excitation beam and a probe beam. Terahertz pulses are generated by optical excitation of a biased photoconductive antenna when illuminated by each laser pulse. Emitted terahertz pulses are collimated and focused onto a sample using a series of off-axis mirrors. Reflected and backscattered terahertz pulses are collected and focused, using a set of off-axis mirrors, onto an unbiased photoconductive antenna for laser-gated terahertz detection. To acquire a TPI map of each paint sample, terahertz reflection waveforms are measured at a point spacing of 200 μm over a 20 mm by 20 mm area. Each time-domain waveform is discretely sampled over 512 data points and can be acquired in less than 50 ms.

C. Mechanical Stylus Profilometer

The thickness of the single layer paint samples of Fig. 3(a) was measured using a stylus profilometer (Talysurf i120, Leicester, U.K.), which uses mechanical contact to measure surface topography. The diamond stylus is moved vertically until it is in contact with the sample surface, which is mounted parallel to the direction of travel of the stylus probe head. The stylus is moved laterally across the sample surface and surface variations, in our case due to paint thickness variation, is recorded as a function of scan position by calculating difference in height between the painted surface and the substrate surface. The resolution of the thickness measurement is 16 nm.

*D. X-Ray Microcomputed Tomography (*XμCT*)*

For further validation of TPI-based thickness prediction, XμCT measurements were made using a Skyscan 1172/F instrument (Skyscan, Konitch, Belgium, control software v1.5.1.3) to image a subset of the four-layer paint sample (both metallic and carbon fiber substrate). The XμCT system used employs cone beam geometry with a fixed CCD array detector. Here the spatial resolution depends mainly on the size of the sample and the resolution of the CCD array (the smaller the sample the higher the resolution). For the measurement a sample with a diameter of 0.635 cm is punched out from the painted panel leading to an isotropic voxel resolution of 2.4 μm in the subsequent XμCT measurements. For each paint sample 796 shadow images were acquired over 180 degree of rotation. Reconstruction of the cross-section images was performed using the program NRcon+GPUReconSever (Skyscan, beta v1.6.5) on a single PC using GPU accelerated reconstruction. The paint sample was rotated to align the center band parallel to the z-axis using DataViewer (Skyscan, v1.4.4). The paint thickness can be obtained from the z-projection maps.

TABLE I
OPTICAL PROPERTIES OF SINGLE LAYER PAINT SAMPLES MEASURED ON MIRROR SUBSTRATE

Optical Properties	Clear-coat	Basecoat			Primer		Electrocoat
		Solid Black[a]	Effect Black[b]	Silver[c]	Primer1	Primer2	
n_{eff}	1.56	1.64	1.73	8.22	2.11	2.61	1.72
κ_{eff}	30	78	140	3880	55	991	84

[a] Black color basecoat without metallic particles.
[b] Black color basecoat with mica particles.
[c] Silver color basecoat with aluminum flakes.

IV. RESULTS

A. Single Paint Layer Samples

One-dimensional (1-D) paint thickness distributions of the single-layer paint samples were measured using the surface profilometer at 0.25 μm steps over a range of 6 mm. Terahertz measurements were acquired subsequently on the same samples. For the TPI measurement an area of 6×6 mm was mapped at a resolution of 0.2 mm per step. The optical properties (the effective refractive index n_{eff} and extinction coefficient κ_{eff}) of the paint samples were calculated from the averaged measured terahertz waveform and the mean paint thickness as measured by the profilometer. Table I summarizes the optical properties of the seven different paint samples studied.

The key characteristic used as a basis for determining paint quality is layer consistency. The big advantage of TPI is that the technique is capable of measuring not only an average thickness but also to resolve the homogeneity of the coating thickness across the entire surface of the sample to determine the uniformity of the paint layer and detect paint defects. Fig. 4(a) and 4(b) shows a comparison of a 1-D thickness profile for a single layer of clearcoat on mirror as measured by profilometer and predicted from terahertz measurements. For both measurement methods the 1-D thickness distribution follows a similar trend and we note that at the edge of the film significant paint defects are observed where poor adhesion leads to paint peeling off the substrate. Such defects are typically caused by incompatible materials either in the paint or on the substrate or improper paint application process control. Terahertz measurements were made however, not over a 1-D trace, but instead over a 2-D area and therefore a map of thickness as a function of position can be generated, as shown in Fig. 4(c). The histogram [Fig. 4(d)] clearly indicates distinctly thickness variations over the entire surface, which is critical factor to determine the quality of the paint layers.

B. Four-Layer Paint Samples on Metallic Substrate

TPI measurements were made on the multi-layer paint samples consisting of four layers of paint on a metallic substrate, as depicted in Fig. 3(b). The sample was raster scanned over a square area of dimensions 10×10 mm. Results of measurements made on two different 4-layer samples (one containing a solid black basecoat and the other a metallic silver basecoat containing aluminum flakes) are shown in Fig. 5. The images in the left (right) column correspond to data acquired from the sample containing solid (metallic) basecoat. The 2-D maps in

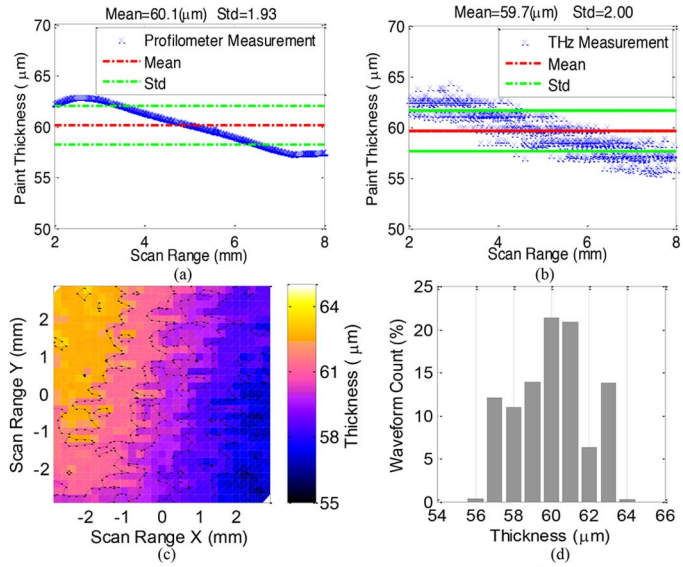

Fig. 4. 1-D thickness profile of a single paint layer (clearcoat) as measured by: (a) profilometer and (b) Terahertz. (c) A 2-D layer thickness map generated from terahertz data. (d) Histogram of coating thickness distribution for a single paint layer.

the first row of Fig. 5, labeled "Peak Intensity", show the magnitude of the most intense reflection peak in the time-domain waveforms recorded over the square area. The B-scans below these 2-D maps show individual waveforms as a function of vertical scan position. Color lines in the B-scan map represent the interface between different paint layers. The third row contains a single measured waveform and the corresponding simulated waveform for the two samples. Finally, the fourth row shows the difference between those measured and simulated waveforms.

It is clear from Fig. 5(a) and 5(e) that there is a greater variation in the strength of reflection from sample containing metallic basecoat. Such variation is caused by the aluminum flakes in the basecoat. Fig. 5(c) and 5(g) shows deconvolved time-domain reflected waveforms form a single point on the sample. For the solid black basecoat sample, the first, second, and third positive reflections are from the air–clearcoat, basecoat–primer1, and electrocoat–metal boundary. Reflection peaks were not seen from the interface between clearcoat–basecoat as well as primer1–electrocoat because of the small refractive index difference between these layers. The sample containing metallic basecoat is challenging because aluminum flakes in the basecoat cause higher reflection and scattering effects. The first two well-resolved positive peaks in the waveform are reflections from the air–clearcoat and clearcoat–basecoat interfaces. They are followed by a negative reflection peak at the basecoat–primer1 interface where a relatively large drop in refractive index occurs. The following positive peak is at the interface between electrocoat–metal substrate. The thickness of each layer corresponds to the simulated reflection waveform (in red) that most closely matches the measured waveform (in blue). Fig. 5(d) and 5(h) shows the residual between the measured and simulated waveforms.

To validate the thickness values predicted from the analysis of the terahertz measurements three reference techniques (eddy current, ultrasound and XμCT) were applied to independently

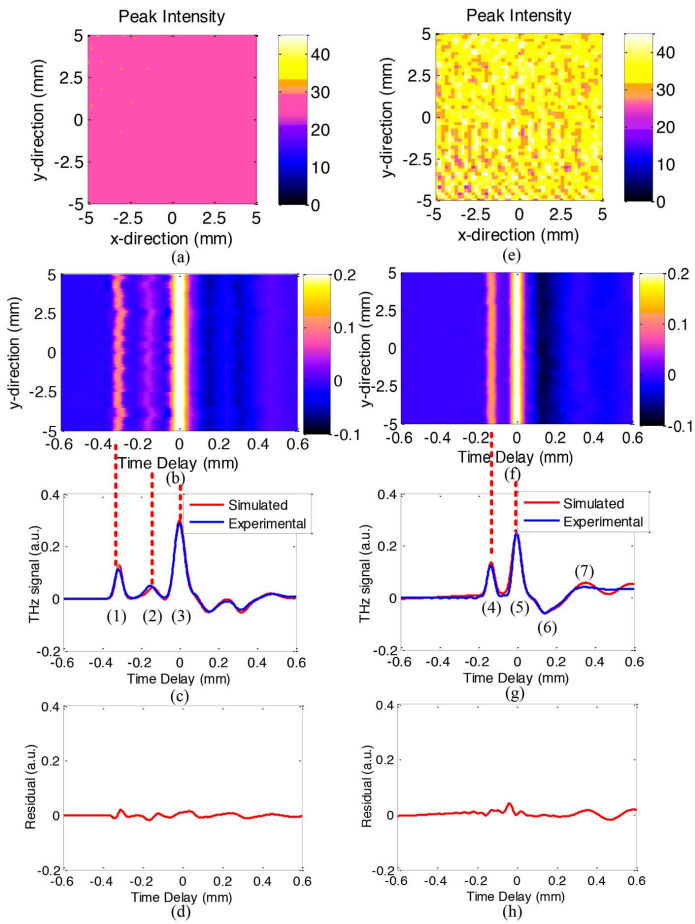

Fig. 5. TPI reflection data from four-layer paint on metallic substrate. Left column: solid black basecoat; right column: metallic basecoat with aluminum flakes. (a), (e) 2-D reflection peak intensity map. (b), (f) B-scan map measured along the y-direction. (c), (g) Time-domain reflection waveform of at a single point in the scanned area. (d), (h) Residual between the measured and simulated waveforms. The labeled reflection peaks corresponds to the following interfaces: (1), (4) air–clearcoat; (2) basecoat(solid black)-primer1; (3), (7) electrocoat-metal substrate; (5) clearcoat–basecoat; (6) basecoat(metallic silver)-primer1.

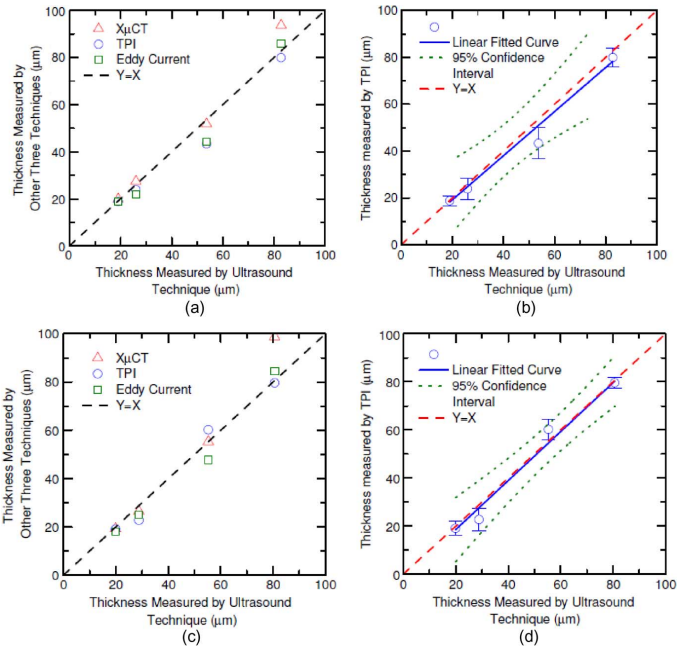

Fig. 6. Coating thickness (eddy current, XμCT and TPI) as a function of thickness measured by ultrasound technique showing results from 4-layer samples containing (a), (b) solid basecoat and (c), (d) metallic basecoat containing aluminum flakes. (From left to right: electrocoat, basecoat, primer1, and clearcoat) Error bars represent standard deviation of thickness measured by TPI.

quantify the thickness of the various paint layers. The eddy current method cannot resolve the individual layer thickness from a stack of layers but merely measures the total thickness of the film build. In order to estimate the thickness of each individual layer using the eddy current meter, a set of stepped samples were prepared using tape layers that were subsequently removed between the application of the paint layers [Fig. 3(d)]. The thickness of the individual layers of the full stack sample is calculated by subtraction, i.e., the thickness of clearcoat is $d_{A2} - d_{A1}$ while the thickness of the basecoat is $d_{A3} - d_{A2}$. In the XμCT measurements there was poor contrast between some of the layers in the stack and the boundaries between basecoat and clearcoat cannot be fully resolved due to this lack of contrast. The thickness of the clearcoat layer was measured by subtracting the thickness of A_1 from A_2. Table II shows the comparison of thickness results measured by the four different methods. Using the ultrasound measurements, which is the most commonly used technique to measure the individual layers in the automotive industry, as our standard, Fig. 6(a) and 6(c) shows the coating thickness measured by the other three methods in comparison for solid and metallic basecoat sample. Compared to the XμCT and eddy current techniques, the thickness measured by TPI shows a better correlation with the ultrasound measurement. Due to the substration calculation process outlined above there can be measurement error of the eddy current meter carried forward from both measurement steps rather than one. The errors from the XμCT measurements are mainly due to the uncertainty of defining the boundary of subsequent layer from reconstructed cross section image. We estimate the error to be 4.8 μm (two pixels size). Fig. 6(b) shows the mean thickness value measured by TPI and the corresponding error bars as a function of thickness measured by ultrasound for solid basecoat sample and Fig. 6(d) shows the relationship for metallic basecoat samples. For both cases the linear fitting line weighted by the error bars and Y = X fitting lines are plotted and fall into the 95% confidence range.

C. Four-Layer Paint Samples on Non-Metallic (Carbon Fiber) Substrate

In addition to measurements made on a metallic substrate, we were able to resolve individual paint layers applied to a carbon fiber substrate [shown in Fig. 3(c)]. The difference in optical properties at each interface is quite large (see Table I). Therefore most reflection peaks (except that at the clearcoat to basecoat boundary) at the interface between paint layers are well separated in time and can be clearly resolved. As shown in Fig. 7, the first, second and fifth positive peaks are reflections from air/clearcoat, basecoat/primer1, and carbon fiber inner structure, respectively. The third and fourth were negative reflections from primer1/primer2 and primer2/carbon fiber substrate interfaces.

TABLE II
PAINT THICKNESS (μm) MEASURED BY TPI, EDDY CURRENT, ULTRASOUND AND XμCT TECHNIQUES FOR A STACK OF PAINT LAYERS DEPOSITED ON A METAL SUBSTRATE

Sample	Technique	Electrocoat	Primer1	Basecoat	Clearcoat	Total
Black[a]	TPI	18.8	43.3	23.9	79.9	165.9
	Eddy Current	18.8	44.1	21.7	85.9	170.5
	Ultrasound	19.0	53.7	25.0	82.8	180.5
	XμCT	19.8	51.8	27.4	93.7	192.7
Silver[b]	TPI	19.0	60.2	22.7	79.6	181.5
	Eddy Current	18.1	47.7	24.9	84.4	175.1
	Ultrasound	19.9	55.3	28.0	80.6	183.8
	XμCT	19.2	55.3	26.4	98.7	199.6

[a] Solid black basecoat: Black color sample without metallic particles;
[b] Metallic silver basecoat: Silver color metallic sample with aluminum flakes.

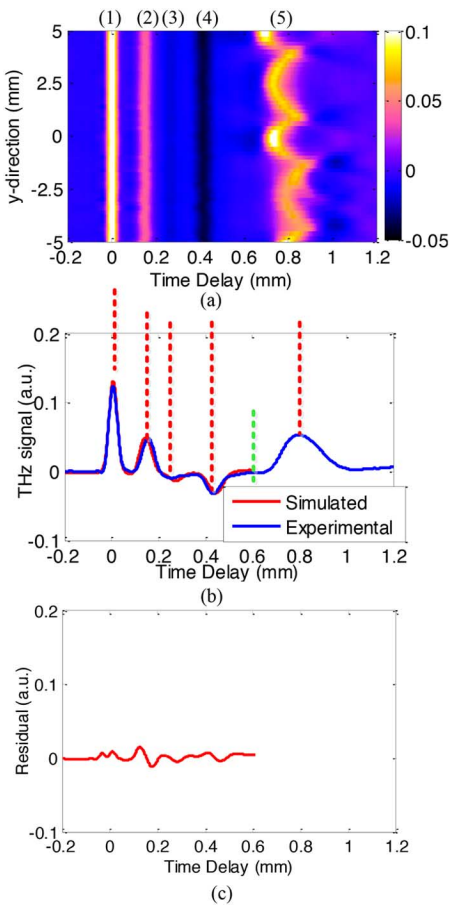

Fig. 7. TPI reflection data of four-layer paint on a non-metallic substrate (carbon fiber) containing effect black basecoat. (a) B-scan map measured along the y-direction. (b) Time-domain reflection waveform of a single pixel. (c) residual between the experimental waveform and simulated waveform. (1) air–clearcoat; (2) basecoat–primer1; (3) primer1–primer2; (4) primer2–front surface of carbon fiber substrate.

Due to the nested structure and nonuniform internal microstructure of the carbon fiber composite substrate, the simulated waveform is only valid to just beyond the front wall of the carbon fiber substrate (indicated by the green dashed line in Fig. 7(b).

The thickness measured by all the three different techniques (TPI, ultrasound, and XμCT) is listed in Table III. Fig. 8(a) shows the coating thickness measured by ultrasound as a function of coating thickness measured by the other two techniques

TABLE III
PAINT THICKNESS (μm) MEASURED BY TPI, ULTRASOUND, AND XμCT TECHNIQUES FOR A STACK OF PAINT LAYERS DEPOSITED ON A CARBON FIBER SUBSTRATE

Sample	Technique	Primer2	Primer1	Basecoat	Clearcoat	Total
Effect Black[a]	TPI	73.8	57.0	22.1	62.2	215.1
	Ultrasound	73.0	52.1	22.0	71.8	221.1
	XμCT	80.9	56.3	26.5	70.3	233.3

[a] Black color basecoat containing mica particles.

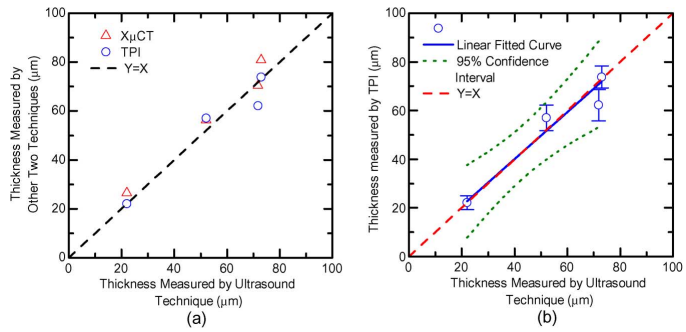

Fig. 8. Coating thickness as measured by TPI and XμCT as a function of thickness measured by ultrasound technique for the individual paint layers of a 4-layer stack containing black effect basecoat on a nonmetallic substrate (from left to right: Basecoat, primer1, clearcoat, and primer2). Error bars represent standard deviation of thickness measured by TPI.

for metallic basecoat sample with carbon fiber substrate. The mean thickness values measured by TPI together with their corresponding error bars as a function of thickness measured by ultrasound are plotted in Fig. 8(b). The weighted linear fitting line and the $Y = X$ line are plotted, both of which fall within the 95% confidence interval. In general, the terahertz measurement shows good agreement with the ultrasound technique. One reason for the slight discrepancy at higher film builds could be due to out-of-focus effects during measurement using the current focal length optics. Another possible explanation for this difference could be that we assume a constant refractive index value across the entire accessible terahertz spectral range. The assumption is reasonable for non-absorbing samples (e.g., clear coat as evident from terahertz spectra of a large number of samples we measured in the past). However, this assumption might be problematic for absorbing samples (e.g., base and primer coats) and further research will have to address this question.

V. CONCLUSION

In summary, we have reported a new approach to measure the individual thickness of paint layers on multi-layered automobile paints panels. Here we have shown that it was possible to measure the layer thickness on both metallic and non-metallic substrates for a range of different basecoat materials (with and without metallic particles). The terahertz results were compared with other techniques (ultrasound measurements, eddy current measurements as well as reconstructed cross sections based on XμCT images) and showed good agreement. The terahertz technique has the advantage of : 1) non-contact measurement compared to traditional tools; 2) suitability for a variety of coating films and substrates; 3) the ability to measure the thickness of individual layers in multi-layered coatings; and 4) the ability to provide maps of thickness distribution over a surface

compared to single point measurements. Furthermore, TPI might have potential for in-line paint thickness measurement and monitoring wet to dry transformation processes.

ACKNOWLEDGMENT

The authors would also like to acknowledge support by the U.K. Engineering and Physical Sciences Research Council (EP/K503721/1).

REFERENCES

[1] J. A. Zeitler and Y. C. Shen, "Industrial applications of terahertz imaging," in *Terahertz Spectroscopy and Imaging*, K. E. Peiponen, J. A. Zeitler, and M. Kuwata-Gonokami, Eds. Berlin, Germany: Springer, 2013, ch. 18, pp. 451–489.

[2] C. D. Stoik, M. J. Bohn, and J. L. Blackshire, "Nondestructive evaluation of aircraft composites using transmissive terahertz time domain spectroscopy," *Opt. Express* vol. 16, no. 21, pp. 17039–17051, 2008.

[3] J. A. Zeitler and L. F. Gladden, "In-vitro tomography and non-destructive imaging at depth of pharmaceutical solid dosage forms," *Eur. J. Pharm. Biopharmacol.* vol. 71, no. 1, pp. 2–22, 2009.

[4] J. A. Zeitler, P. F. Taday, D. A. Newnham, M. Pepper, K. C. Gordon, and T. Rades, "Terahertz pulsed spectroscopy and imaging in the pharmaceutical setting—A review," *J. Pharm. Pharmacol.* vol. 59, no. 2, pp. 209–223, 2007.

[5] R. K. May, K. Su, L. Han, S. Zhong, J. A. Elliott, L. F. Gladden, M. Evans, Y. C. Shen, and J. A. Zeitler, "Hardness and density distributions of pharmaceutical tablets measured by terahertz pulsed imaging," *J. Pharm. Sci.* vol. 102, no. 7, pp. 2179–2186, 2013.

[6] J. F. Federici, B. Schulkin, F. Huang, D. Gary, R. Barat, F. Oliveira, and D. Zimdars, "THz imaging and sensing for security applications-explosives, weapons and drugs," *Semicond. Sci. Technol.* vol. 20, no. 7, pp. S266–S280, 2005.

[7] Z.-H. Michalopoulou, S. Mukherjee, Y. Hor, K. Su, Z. Liu, R. Barat, D. Gary, and J. Federici, "RDX detection with THz spectroscopy," *J. Infrared, Millim., THz Waves* vol. 31, no. 10, pp. 1171–1181, 2010.

[8] T. Yasui, T. Yasuda, K. Sawanaka, and T. Araki, "Terahertz paintmeter for noncontact monitoring of thickness and drying progress in paint film," *Appl. Opt.* vol. 44, no. 32, pp. 6849–6856, 2005.

[9] T. Yasuda, T. Iwata, T. Araki, and T. Yasui, "Improvement of minimum paint film thickness for THz paint meters by multiple-regression analysis," *Appl. Opt.* vol. 46, no. 30, pp. 7518–7526, 2007.

[10] D. M. Mittleman, S. Hunsche, L. Boivin, and M. C. Nuss, "T-ray tomography," *Opt. Lett.* vol. 22, no. 12, pp. 904–906, 1997.

[11] Y. C. Shen and P. F. Taday, "Development and application of terahertz pulsed imaging for nondestructive inspection of pharmaceutical tablet," *IEEE J. Sel. Topics Quantum Electron.*, vol. 14, no. 2, pp. 407–415, Mar./Apr. 2008.

[12] S. N. Taraskin, S. I. Simdyankin, S. R. Elliott, J. R. Neilson, and T. Lo, "Universal features of terahertz absorption in disordered materials," *Phys. Rev. Lett.* vol. 97, p. 055504, 2006.

[13] Y. C. Shen, P. F. Taday, and M. Pepper, "Elimination of scattering effects in spectral measurement of granulated materials using terahertz pulsed spectroscopy," *Appl. Phys. Lett.*, vol. 92, no. 5, p. 051103, 2008.

[14] J. A. Zeitler, Y. C. Shen, C. Baker, P. F. Taday, M. Pepper, and T. Rades, "Analysis of coating structures and interfaces in solid oral dosage forms by three dimensional terahertz pulsed imaging," *J. Pharm. Sci.* vol. 96, no. 2, pp. 330–340, 2007.

Ke Su received the B.S. degree in applied physics from the University of Zhengzhou, China, in 2003, the M.S. degree in material science from Fudan University, China, in 2006, and the Ph.D. degree in applied physics from New Jersey Institute of Technology, Newark, NJ, USA, in 2011. Her doctoral research concerned Terahertz communication and Terahertz synthetic aperture imaging.

She is currently a Research Associate in the Terahertz Applications Group at the University of Cambridge, Cambridge, U.K. Her research interests include THz application on coating measurement, THz imaging and THz spectroscopy.

Yao-Chun Shen is a Senior Lecturer at the Department of Electrical Engineering and Electronics, University of Liverpool, Liverpool, U.K., since June 2007. Before that he has worked on terahertz-related technology for many years, first as a Research Associate at the Cavendish Laboratory, University of Cambridge, Cambridge, U.K., and then as a Senior Scientist at TeraView Limited, Cambridge, U.K. He has been awarded seven terahertz-related patents, and published over 80 peer-reviewed journal papers that are highly cited with an *h*-index of 23. His current research interests include the development of novel terahertz devices and imaging techniques and, in particular, its industrial applications

J. Axel Zeitler received the undergraduate degree from the University of Wurzburg, Germany, and the Ph.D. degree from the University of Otago, New Zealand.

He is a University Lecturer at the Department of Chemical Engineering and Biotechnology, University of Cambridge, U.K., where he leads the Terahertz Applications Group. He is a Fellow at Gonville and Caius College, where he was a Research Fellow prior to his current appointment. In addition to his university position, he holds a College Lectureship in Chemical Engineering, as well as in Chemistry. He has held research positions at the Cavendish Laboratory, University of Cambridge, U.K., and TeraView Ltd., Cambridge, U.K.